

---

# METCC: METric learning for Confounder Control

## Making distance matter in high dimensional biological analysis

---

**Kabir Manghnani**

kabir.manghnani@freenome.com  
kabirm2@illinois.edu

**Adam Drake**

adam.drake@freenome.com

**Nathan Wan**

nwan@freenome.com

**Imran S. Haque**

ihaque@cs.stanford.edu

### Abstract

High-dimensional data acquired from biological experiments such as next-generation sequencing are subject to a number of confounding effects. These effects include both technical effects, such as variation across batches from instrument noise or sample processing ("batch effects"), or institution-specific differences in sample acquisition and physical handling ("institutional variability"), as well as biological effects arising from true but irrelevant differences in the biology of each sample, such as age biases in diseases. Prior work has used linear methods to adjust for such batch effects. Here, we apply contrastive metric learning by a non-linear triplet network to optimize the ability to distinguish biologically distinct sample classes in the presence of irrelevant technical and biological variation. Using whole-genome cell-free DNA data from 817 patients, we demonstrate that our approach, METric learning for Confounder Control (METCC), is able to match or exceed the classification performance achieved using a best-in-class linear method (HCP) or no normalization. Critically, results from METCC appear less confounded by irrelevant technical variables like institution and batch than those from other methods even without access to high quality metadata information required by many existing techniques; offering hope for improved generalization.

## 1 Introduction

The acquisition of biological data, such as DNA sequencing, requires complex and inter-dependent procedures that are sensitive to variables that are not of interest to the data's user [1]. Numerous factors, including but not limited to sample processing, storage time, and temperature, all affect the simultaneous measurement of thousands to millions of variables in DNA sequencing. These confounders pose a challenge when developing solutions to pattern recognition problems using biological data because they can obscure the biological signal of interest.

Accounting for and normalizing technical variables from data has a rich history dating back at least 100 years to RA Fisher's work on ANCOVA and random effects [2], [3]. Many normalization methods are derived from this initial formulation that models the response variable as a function of both global and group level parameters. These models specify a mean effect parameter to be estimated per group that accounted for unwanted group-wise variation of the mean. More flexible models have been developed: mixed effects models, for example, fit a set of global and group indexed parameters [4]–[6]. In particular, HCP (Hidden Covariates with Prior) models the normalized data,

$\hat{Y}$ , as  $N(\hat{Y}|XW + FB, I)$  where  $F$  is a matrix of known covariates,  $X$  is a matrix of unknown covariates, and  $W$ ,  $B$ , and  $X$  are estimated from the data [6]. Depending on the hyperparameters, this model subsumes model specification similar to two popular normalization models: ComBat [4] and PANAMA [7]. Separately, there are efforts in to estimate data representations that are invariant with respects to technical effects. For example, Shaham et al. normalizes confounder effects in RNA sequencing using a variational adversarial approach [8]. The application of their method is unfortunately limited to pairs of batches.

Unlike previous models, we approach the covariate normalization problem as a reduced representation learning problem using methods of blackbox metric learning such as siamese and triplet networks [9], [10]. By enforcing a learned metric with a loss function aiming to preserve biological information we learn a representation that contains less of the variation due to confounding effects. Metric learning methods are advantageous because the loss function requires only the variable of interest as opposed to mixed effects models which also require annotation of the technical effects to normalize. Additionally our method provides the ability to model non-linear effects unlike that of HCP.

We analyze 1) the extent to which data normalized with HCP and METCC retains information about the unwanted technical effects and 2) the performance of supervised models trained on normalized data.

## 2 Methods

### 2.1 METCC learning

Let  $X$  be an  $n \times p$  matrix of observed biological data with  $n$  samples and  $p$  measurements. Let  $y$  be a biological variable of interest such as phenotype label or disease status. We seek to learn a distance function  $D_w$  parameterized by the map  $g : \mathbb{R}^p \rightarrow \mathbb{R}^k$  where the distance between 2 samples  $x_i$  and  $x_j$  is determined by  $D_w = \|g(x_i) - g(x_j)\|_2$ . The objective is to transform the data with  $g$  so that the variability measured between sample  $x_i$  and  $x_j$  is low when  $y_i = y_j$  and high when  $y_i \neq y_j$ . This can be optimized using a contrastive, or siamese, loss function proposed by Hadsell et al. [9],

$$\operatorname{argmin}_w (1 - L)D_w(x_i, x_j)^2 + (L)\max(0, m - D_w(x_i, x_j))^2 \quad (1)$$

where  $L = 0$  if  $y_i \neq y_j$ ,  $L = 1$  otherwise, and  $m$  is a fixed margin. Equation (1) can be described as follows, the first term of the loss function encourages samples from the same class but different institutes to be close in the latent space; while the second penalizes samples from the same institute that remain close in the latent space while belonging to different disease classes.

This has been extended and shown to produce better representations when both a positive and negative class sample are used for each anchor sample. Hoffer and Ailon proposed a triplet loss that extends equation (1) by running a triplet of samples  $(x^-, x, x^+)$  through  $D_w$  where  $x$  is an anchor sample,  $x^-$  is from a different and  $x^+$  is from the same class [10]. The distances obtained are  $d_+ = D_w(x, x^+)$  and  $d_- = D_w(x, x^-)$  and the loss function minimized is,

$$\operatorname{argmin}_w \|d_+, d_- - 1\|_2^2 \quad (2)$$

This loss function poses the metric learning task as classifying  $x^+$  and  $x^-$  as either being a member of the  $x$  class or not.

Hoffer and Ailon suggest a distance function defined with a softmax on the outputs  $D_w$  [10]; we instead use the formulation of Balnter et al. that forgoes the softmax [11].

In practice, the biological data coming off of a sequencer can have tens of thousands of measured variables. In order to obtain a stable solution to equations (1) or (2) with gradient descent we found that unsupervised dimensionality reduction techniques like principal components analysis (PCA) need to be applied to  $X$  prior to metric learning likely due to our relatively limited sample size. We trained  $D_w$  where  $X$  was a matrix of cfDNA data and  $y$  was a label to predict.

### 2.2 Classifications

Once  $D_w$  is trained we take the output of  $g(\cdot)$  as the METCC embedding for each sample (see workflow in Figure 1). In order to assess the quality of these METCC embeddings, separate embeddings

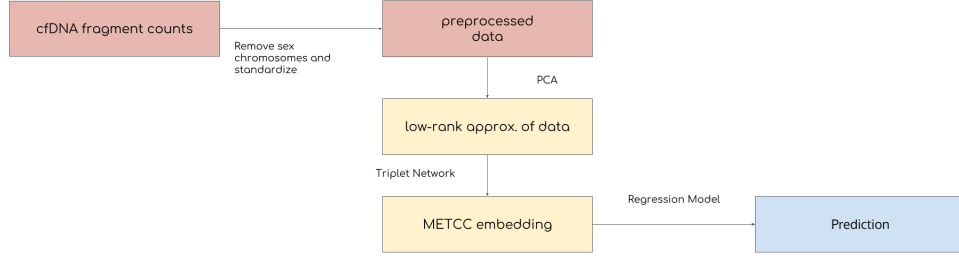


Figure 1: METCC data workflow

are also constructed from baseline methods of PCA and HCP from the same samples, and all three embeddings are subsequently used to train both a k-nearest neighbor (KNN) and a logistic regression (LR) model to predict disease with k-fold cross validation ( $k = 4$ ) [12]. In order to assess the confounder signals in the embeddings, regression models are also trained with confounder values as the target label.

### 3 Experiments and results

Our dataset is a collection of 817 cell-free DNA (cfDNA) samples and their associated metadata [13]. The raw data  $X$  consists of the number of DNA fragments overlapping each gene annotated in the CHES gene set consisting of 24152 gene features for each sample [14]. All samples were sequenced to approximately 10x depth (i.e., each base in the genome appeared, on average, in approximately 10 independent fragments). Each sample is labeled as coming from an individual with colorectal cancer or from a healthy individual. Positive labels were confirmed by colonoscopy and expert analysis of pathology or histology reports.

#### 3.1 Generating Embeddings

In order to assess the quality of METCC embeddings, we prepared two other embeddings to compare against:

$$\begin{aligned}
 X_{PCA} &= PCA(x) \\
 X_{HCP} &= PCA(HCP(X)) \\
 X_{METCC} &= METCC(PCA(X))
 \end{aligned} \tag{3}$$

Before  $X$  is transformed a basic pre-processing step is applied to the raw data that removes sex chromosomes and standardizes each sample. We apply PCA after HCP in order to have comparable dimensions for the data used when training a classifier.  $X_{PCA}$  is a baseline comparator with no additional normalization, just dimensionality reduction with PCA.  $X_{HCP}$  is embedding normalized with HCP using only institution, batch, and age labels. The institution reflects the provenance of the patient’s sample. The batch entails the sequencing chemistry preparation and process and thus reflects both short and long term effects in the data. We grouped age into the bins: [0-50, 50-55, 55-60, 60-75, 75-80, 80-85, 85+].  $X_{METCC}$  is the METCC embedding that is the result of the method described in 2.1. METCC has no knowledge of any confounders, only the disease label. Hyperparameters for HCP and METCC were selected by choosing the best performing logistic regression model across a random search of the normalization methods’ hyperparameters and regularization of the logistic regression model (see section 5.2). Regularization for all logistic regression models including confounder tasks were performed independently.

Manifolds of these embeddings are plotted by various targets in section 5.3.

#### 3.2 Classification and embedding analysis

For each set of embeddings in section 3.1, we first classify by disease label, the target of biological interest. The mean of the Area Under the Receiver Operating Characteristics (AUROC) for each

Normalization	Train AUC (KNN)	Test AUC (KNN)	Train AUC (LR)	Test AUC (LR)
PCA-only	$0.87 \pm 0.0080$	$0.79 \pm 0.036$	$0.97 \pm 0.0024$	$0.92 \pm 0.013$
HCP	$0.90 \pm 0.0079$	$0.82 \pm 0.040$	$0.99 \pm 0.0013$	$0.91 \pm 0.012$
METCC	$1.00 \pm 0.00032$	<b><math>0.87 \pm 0.023</math></b>	$1.00 \pm 0.00067$	$0.92 \pm 0.0096$

Table 1: Mean k-fold AUROC of disease label classification for different normalization techniques using K-nearest neighbors (KNN) and logistic regression (LR) across folds.

Normalization	Train ACC (KNN)	Test ACC (KNN)	Train ACC (LR)	Test ACC (LR)
PCA-only (inst)	$0.53 \pm 0.0042$	$0.24 \pm 0.027$	$0.82 \pm 0.0065$	$0.30 \pm 0.053$
HCP (inst)	$0.54 \pm 0.018$	$0.20 \pm 0.051$	$0.90 \pm 0.0054$	$0.31 \pm 0.046$
METCC (inst)	$0.50 \pm 0.0076$	$0.23 \pm 0.073$	<b><math>0.38 \pm 0.0095</math></b>	<b><math>0.22 \pm 0.094</math></b>
PCA-only (batch)	$0.29 \pm 0.0063$	$0.062 \pm 0.030$	$0.64 \pm 0.016$	$0.086 \pm 0.018$
HCP (batch)	$0.19 \pm 0.028$	$0.037 \pm 0.0024$	$0.90 \pm 0.0055$	$0.093 \pm 0.0033$
METCC (batch)	$0.22 \pm 0.014$	$0.071 \pm 0.019$	<b><math>0.12 \pm 0.011</math></b>	<b><math>0.058 \pm 0.012</math></b>
PCA-only (age)	$0.37 \pm 0.010$	$0.12 \pm 0.018$	$0.62 \pm 0.0073$	$0.12 \pm 0.038$
HCP (age)	$0.28 \pm 0.030$	$0.15 \pm 0.039$	$0.75 \pm 0.0059$	$0.14 \pm 0.041$
METCC (age)	$0.31 \pm 0.0075$	$0.12 \pm 0.0087$	$0.23 \pm 0.010$	$0.13 \pm 0.044$

Table 2: Mean k-fold accuracy of confounder label classification for institution (inst), batch, and age for different normalization techniques using K-nearest neighbors (KNN) and logistic regression (LR) across folds.

test fold is used as an estimate for performance. As shown previously [13], logistic regression can perform very well on this task, even with just PCA; METCC performs comparably when using logistic regression, but definitely stands out when using a non-parametric, KNN model ( $k = 21$ , selected by minimizing the difference in train/test accuracy).

In addition to disease label classification, we also assess the signal of confounders described in section 3.1 (plotted in Figure 2) by training classifiers using the confounders as the target label value. Since this is no longer a binary classification problem, performance is measured by mean accuracy. Although sometimes subtle, embeddings produced by METCC are significantly more difficult to predict confounders on when the confounder is technical, that is either institution or batch; the removal of unwanted signal is evident across both regression methods. The difference between the normalization methods is not dramatic for age, but from the confounder distribution it is clear that an increase in age is correlated with increased likelihood of disease.

## 4 Discussion and conclusion

We propose the use of a blackbox metric learning method for confounder normalization that accounts for confounder effects without the necessity of having *a priori* knowledge of these effects, which can be rare or hard to procure. METCC can outperform data minimally pre-processed and data normalized with a mixed effects model in a biological prediction task as measured by AUROC (Table 1). We analyzed the data above in confounder prediction tasks in order to measure a proxy for preserved covariate signal in the data (Table 2) and observed that the minimally pre-processed and data normalized with HCP consistently predict at or better than METCC. This indicates that METCC may be abrogating more of the confounder’s effects than compared methods.

Our work demonstrates the feasibility of mitigating non-linear interactions in data that do not facilitate solving a desired pattern recognition task in high dimensional biological data. Future studies will compare black box metric learning models to non-linear mixed effects models as well as assessing more directly the removal of confounder effect and the highlighting of biological signal in learned transformations.

## Acknowledgments

The authors gratefully acknowledge Signe Fransen, Girish Putcha and all colleagues at Freenome for their extensive suggestions, feedback, and editorial support.

## References

- [1] *Purification of total dna from crude lysates using the dneasy blood and tissue kit*, version DY15, Qiagen, Aug. 2006.
- [2] B. Day and R. Fisher, “The comparison of variability in populations having unequal means. an example of the analysis of covariance with multiple dependent and independent variates.”, *Annals of Eugenics*, vol. 7, pp. 338–348, 1937.
- [3] R. Fisher, “The correlation between relatives on the supposition of mendelian inheritance”, *Transactions of the Royal Society of Edinburgh*, vol. 52, pp. 399–433, 1918.
- [4] W. E. Johnson, C. Li, and A. Rabinovic, “Adjusting batch effects in microarray expression data using empirical bayes methods”, *Biostatistics*, vol. 8, no. 1, pp. 118–127, 2007. DOI: 10.1093/biostatistics/kxj037. [Online]. Available: <http://dx.doi.org/10.1093/biostatistics/kxj037>.
- [5] J. Listgarten, C. Kadie, E. E. Schadt, and D. Heckerman, “Correction for hidden confounders in the genetic analysis of gene expression”, *Proceedings of the National Academy of Sciences of the USA*, pp. 16 465–16 470, Feb. 2010.
- [6] S. Mostafavi, A. Battle, X. Zhu, *et al.*, “Normalizing rna-sequencing data by modeling hidden covariates with prior knowledge”, *PLOS ONE*, vol. 8, no. 7, pp. 1–10, Jul. 2013. DOI: 10.1371/journal.pone.0068141. [Online]. Available: <https://doi.org/10.1371/journal.pone.0068141>.
- [7] N. Fusi, O. Stegle, and N. Lawrence, “Joint modeling of confounding factors and prominent genetic regulators provides increased accuracy in genetical genomics studies”, vol. 8, 2012.
- [8] U. Shaham, “Batch effect removal via batch-free encoding”, *BioRxiv*, 2018. [Online]. Available: <http://dx.doi.org/10.1101/380816>.
- [9] R. Hadsell, S. Chopra, and Y. LeCun, “Dimensionality reduction by learning an invariant mapping”, in *2006 IEEE Computer Society Conference on Computer Vision and Pattern Recognition (CVPR’06)*, vol. 2, Jun. 2006, pp. 1735–1742. DOI: 10.1109/CVPR.2006.100.
- [10] E. Hoffer and N. Ailon, “Deep metric learning using triplet network”, *CoRR*, vol. abs/1412.6622, 2014. arXiv: 1412.6622. [Online]. Available: <http://arxiv.org/abs/1412.6622>.
- [11] V. Balntas, E. Riba, D. Ponsa, and K. Mikolajczyk, “Learning local feature descriptors with triplets and shallow convolutional neural networks”, *The British Machine Vision Conference*, pp. 119.1–119.11, 2016.
- [12] F. Pedregosa, G. Varoquaux, A. Gramfort, *et al.*, “Scikit-learn: Machine learning in Python”, *Journal of Machine Learning Research*, vol. 12, pp. 2825–2830, 2011.
- [13] N. Wan, D. Weinberg, T.-y. Liu, *et al.*, “Machine learning enables detection of early-stage colorectal cancer by whole-genome sequencing of plasma cell-free dna”, *BioRxiv*, 2018. DOI: 10.1101/478065. eprint: <https://www.biorxiv.org/content/early/2018/11/24/478065.full.pdf>. [Online]. Available: <https://www.biorxiv.org/content/early/2018/11/24/478065>.
- [14] M. Pertea, A. Shumate, G. Pertea, *et al.*, “Thousands of large-scale rna sequencing experiments yield a comprehensive new human gene list and reveal extensive transcriptional noise”, *BioRxiv*, 2018. DOI: 10.1101/332825. [Online]. Available: <https://www.biorxiv.org/content/early/2018/05/28/332825>.

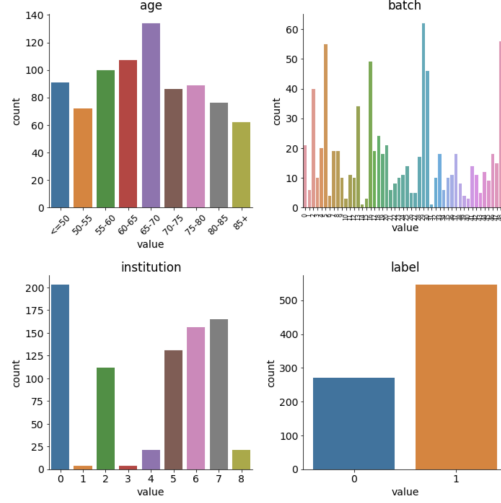


Figure 2: Confounder label distribution

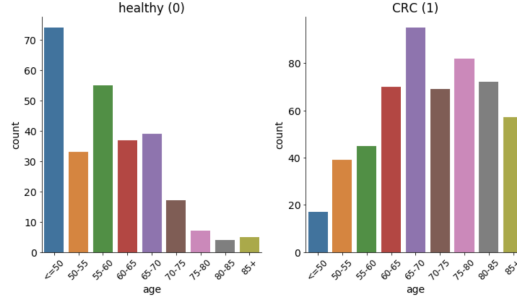


Figure 3: Age bin distribution split by class label

## 5 Supplemental materials

### 5.1 Label distribution

The distribution of samples is not uniform across the disease labels nor the confounders. In this dataset, there are more colorectal samples than not. There is a total of 9 institutions and 50 batches. Note the stark differences in the distribution of ages in Figure 3.

### 5.2 Hyperparameter selection

We selected hyperparameters for HCP and METCC by running a small grid search over a held-out data set. For HCP we swept over the regularization parameters of  $B$ , the number of components in the unknown covariate matrix,  $X$ , and the contribution of the  $XW$  and  $FB$  term to the loss function. For METCC all networks analyzed consisted of a hidden layer of ReLU neurons. The number of neurons and dropout probability were analyzed.

### 5.3 Visualization of embeddings

We applied TSNE to the embeddings  $X_{PCA}$ ,  $X_{HCP}$ ,  $X_{METCC}$  [12]. We colored the projected data by the disease sample (Figure 4), as well as by the confounders being assessed, institution (Figure 5), batch (Figure 6) and age (Figure 7).

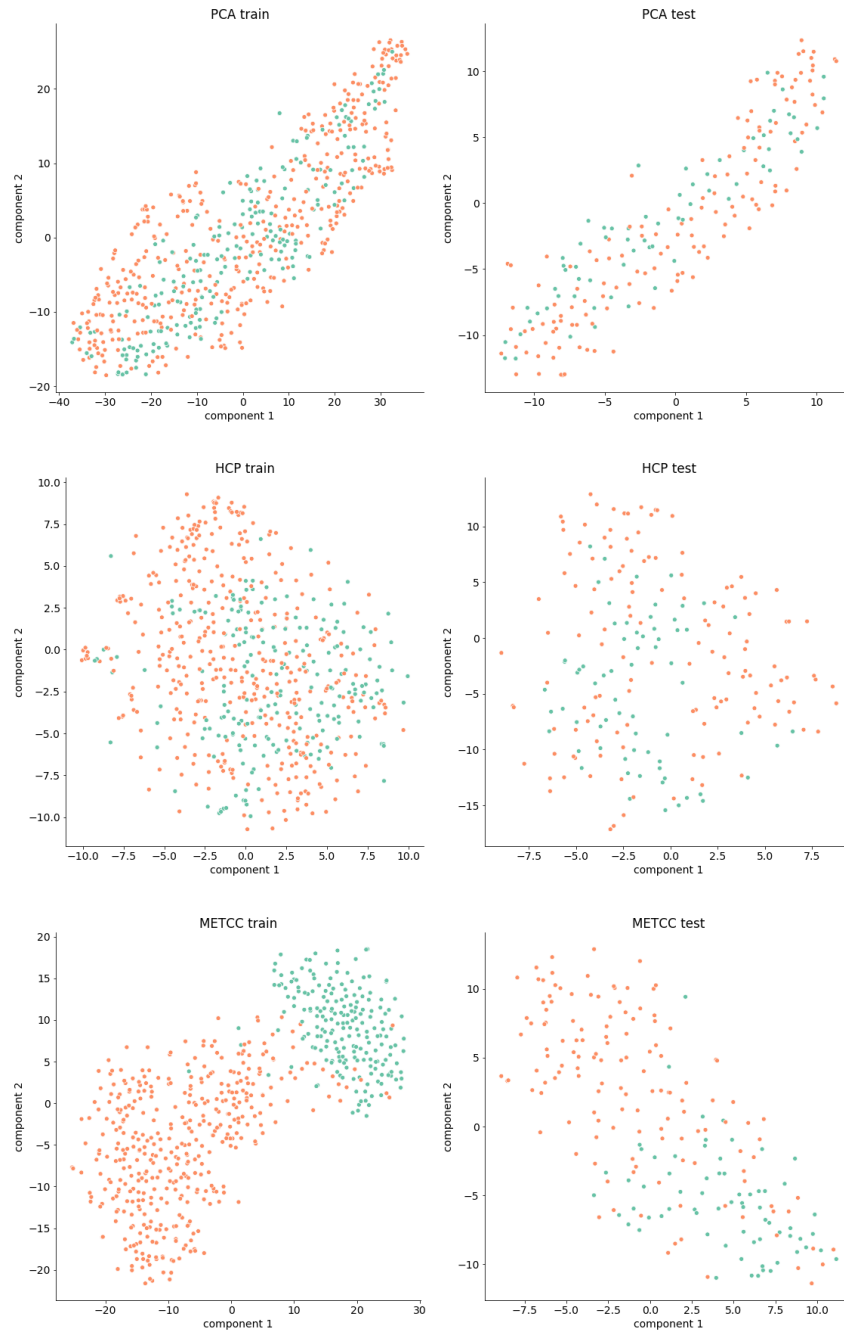


Figure 4: Separate TSNE of train and test sets for one of the folds for each embedding with sample's label indicated by color. Note the clear separation with METCC.

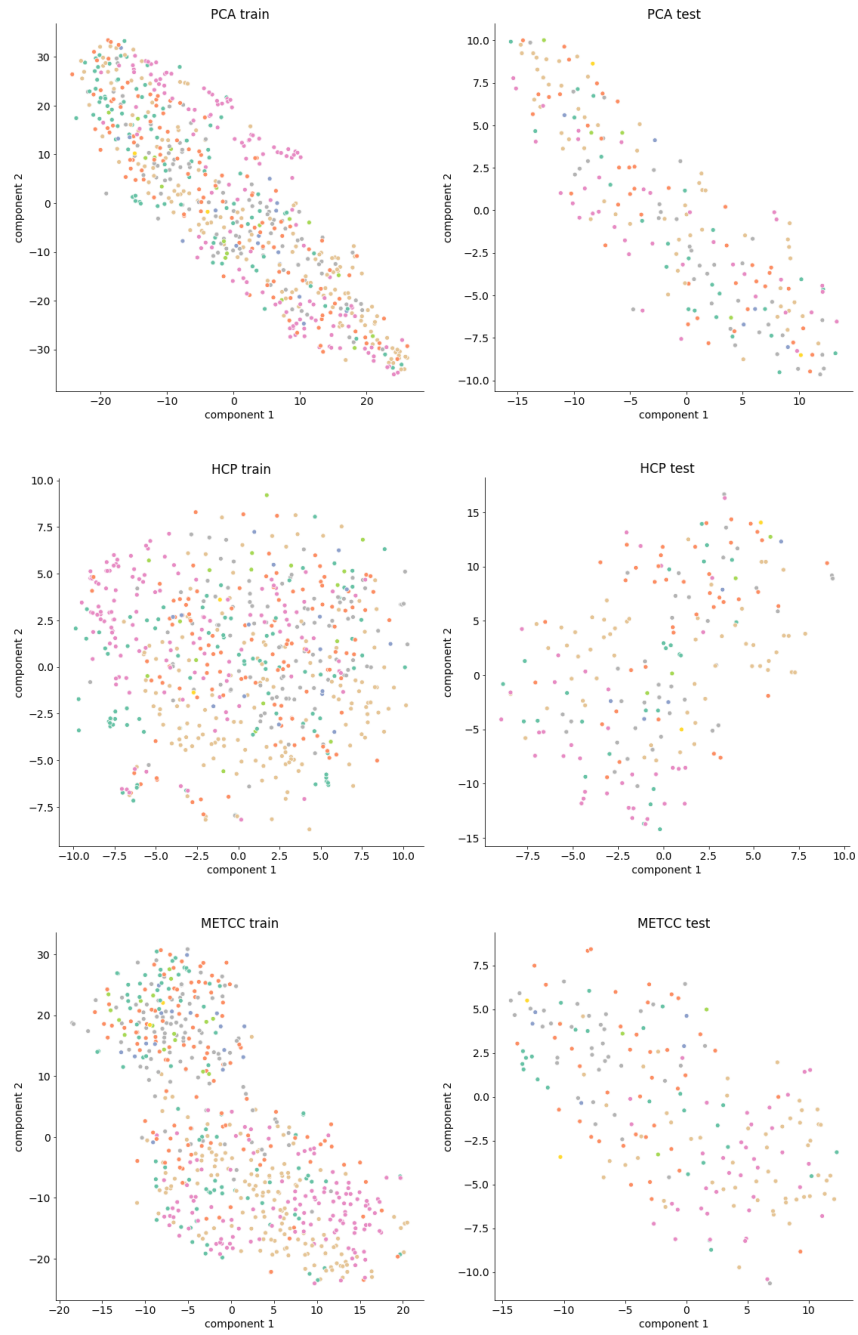


Figure 5: Separate TSNE of train and test sets for one of the folds for each embedding with sample's institution indicated by color. Separability here could indicate confounding signal.



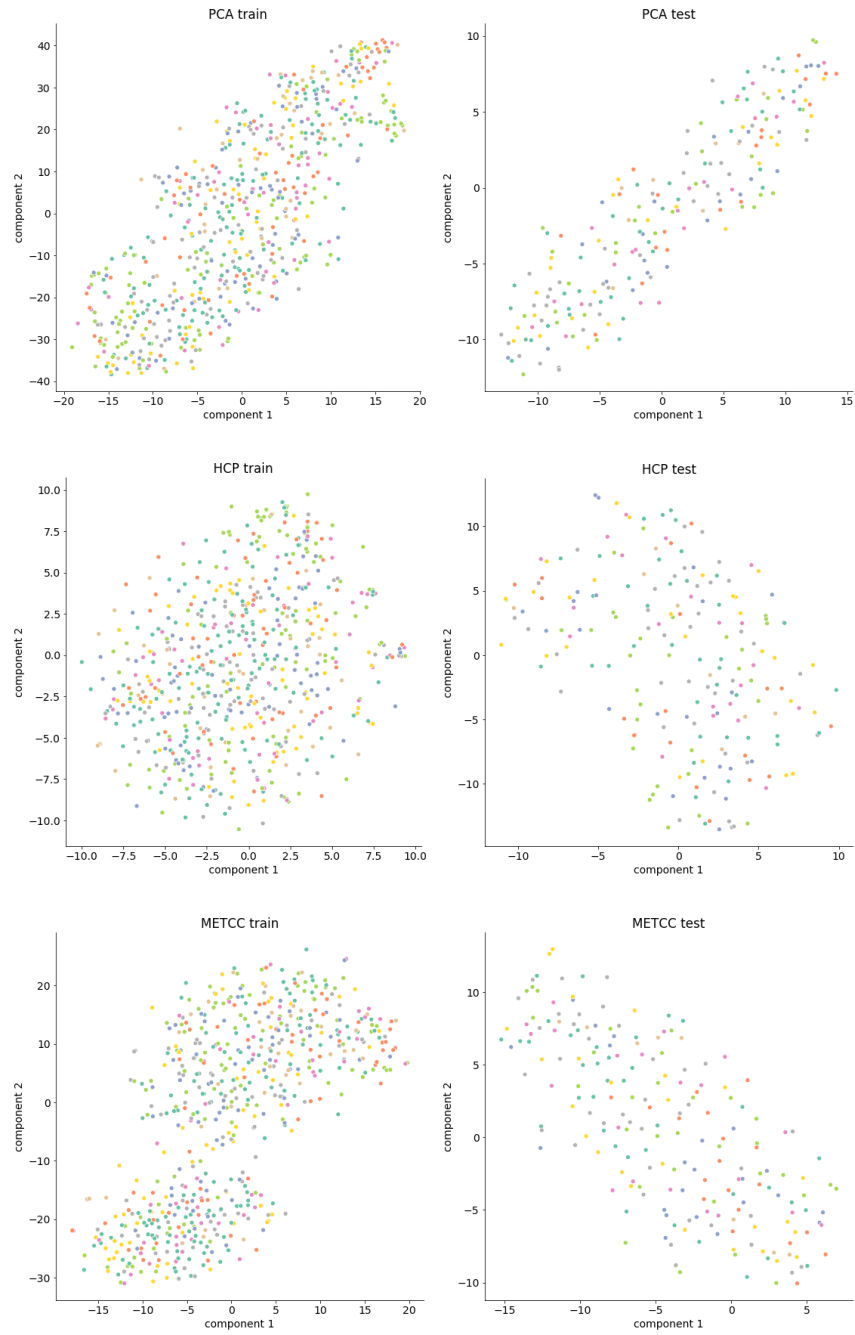


Figure 6: Separate TSNE of train and test sets for one of the folds for each embedding with sample's batch indicated by color. Separability here could indicate confounding signal.

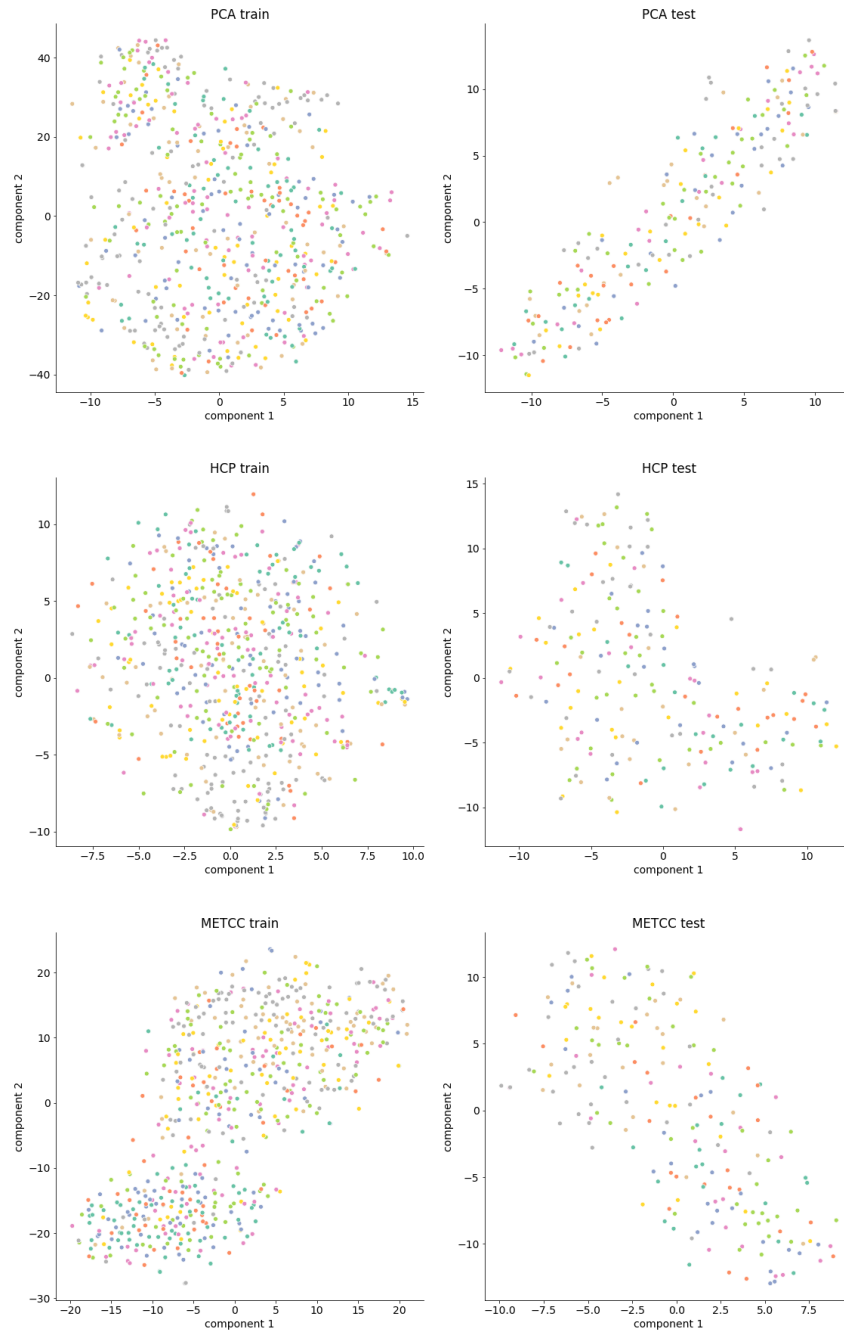


Figure 7: Separate TSNE of train and test sets for one of the folds for each embedding with sample's age bin indicated by color. Separability here could indicate confounding signal.